PNAS RESEARCH ARTICLE | PHYSICS ECONOMIC SCIENCES OPEN ACCESS

Opinion dynamics in financial markets via random networks

Mateus F. B. Granha[a], André L. M. Vilela[a,b,1], Chao Wang[c,1], Kenric P. Nelson[d], and H. Eugene Stanley[b]

Edited by Jose Scheinkman, Columbia University, New York, NY; received January 29, 2022; accepted October 17, 2022

We investigate financial market dynamics by introducing a heterogeneous agent-based opinion formation model. In this work, we organize individuals in a financial market according to their trading strategy, namely, whether they are noise traders or fundamentalists. The opinion of a local majority compels the market exchanging behavior of noise traders, whereas the global behavior of the market influences the decisions of fundamentalist agents. We introduce a noise parameter, q, to represent the level of anxiety and perceived uncertainty regarding market behavior, enabling the possibility of adrift financial action. We place individuals as nodes in an Erdös-Rényi random graph, where the links represent their social interactions. At any given time, individuals assume one of two possible opinion states ± 1 regarding buying or selling an asset. The model exhibits fundamental qualitative and quantitative real-world market features such as the distribution of logarithmic returns with fat tails, clustered volatility, and the long-term correlation of returns. We use Student's t distributions to fit the histograms of logarithmic returns, showing a gradual shift from a leptokurtic to a mesokurtic regime depending on the fraction of fundamentalist agents. Furthermore, we compare our results with those concerning the distribution of the logarithmic returns of several real-world financial indices.

econophysics | sociophysics | Monte Carlo simulation | phase transitions | complex networks

Significance

Financial markets reflect the economic activity of nations, industries, companies, and societies. The recent housing market crash, COVID-19 pandemic, high inflation indices, and cryptocurrency frenzy have illustrated the decisive influence of such systems in modern culture. This work uses an agent-based model within the framework of a complex network to describe asset price dynamics in stock markets. We assume that a financial market comprises two main categories of investors—noise traders and fundamentalists—with the former investing based on its acquaintances and the latter acting based on the market index. Our model reproduces real-world market features for a finite level of social anxiety, denoted by a social temperature, and for a small number of interacting fundamentalist agents in a random network.

We propose the investigation of the influence of random graph networks on the evolution of financial market quantity measures. Inspired by the global-vote model for financial markets (1, 2), we employ an opinion formation model to investigate the underlying socioeconomic mechanisms that drive the behavior of interacting agents within the framework of a complex network. In this context, we consider three primary elements to represent the key features of modern financial markets: agents with different economic strategies that depend on social exchanges, a random network of financial interactions, and a finite level of socioeconomic anxiety.

This presentation illustrates the effectiveness of statistical mechanics methods and techniques as compelling elements through which to understand financial dynamics as a complex system, where agent-based models significantly contribute to revealing intense emergent collective phenomena (3–9). We focus our investigation on an opinion-based exchange that may guide agents' actions in financial markets since it condenses several human behavior-related factors, such as beliefs, moral and religious standards, and social and economic preferences (10–15).

The majority-vote model (MVM) with noise was proposed by Oliveira (16, 17) to investigate opinion dynamics in a society and consists of a sociological adaptation of a magnetic spin model that presents critical behavior similar to that of the Ising model. Lima et al., (18) Campos et al., (19) and Pereira et al. (20) investigated the effects of complex networks on the MVM social dynamics, revealing an ordered phase over the increasing complexity of these networks, while Vilela et al. (1) incorporated the rational and emotional behavior of agents in financial markets, introducing the global-vote model, inspired by the majority-vote dynamics.

The MVM consists of a comprehensive approach to the study of social dynamics with interactions embedded in both regular and complex networks (16–25). In this agent-based model with two states, an individual's opinion at a given time point may assume one of two values, ± 1, regarding some social discussion. Furthermore, an agent in the social network assumes the opinion of the majority of its neighboring spins with probability $(1 - q)$ and the opposite opinion with probability q. The variable q denotes the noise parameter of the model and measures the social unrest or social temperature of the system. The MVM exhibits a second-order phase transition for a critical noise value, $q = q_c \approx 0.075$, for square lattice networks of social interactions (16, 17).

We highlight previous studies regarding the effects of time dependence, agent influence, and economic strategy on financial markets. Hong and Stein developed research

Author contributions: A.L.M.V. and C.W. designed research; M.F.B.G., A.L.M.V., and K.P.N. performed research; A.L.M.V. contributed new reagents/analytic tools; M.F.B.G., A.L.M.V., C.W., and K.P.N. analyzed data; and M.F.B.G., A.L.M.V., C.W., and H.E.S. wrote the paper.

The authors declare no competing interest.

This article is a PNAS Direct Submission.

[1]To whom correspondence may be addressed. Email: chaowanghn@vip.163.com or andre.vilela@upe.br.

Published November 29, 2022.

on underreaction, momentum trading, and overreaction in asset markets by modeling a system populated by two groups of bounded agents—news watchers and momentum traders—driven by one primitive type of shock, slowly diffusing news about future fundamentals (26). The dynamics of speculative behavior were explored by Chiarella, where the presence of two investment strategies was shown to yield exuberant time-dependent phenomena and nonlinearities around the random walk equilibrium price (27). Moreover, Beja and Goldman investigated the price dynamics in disequilibrium and price trends by considering that the demands of investors force market changes and that the speed of price adjustment is finite (28). Such studies encompass relevant nonstationary evolution mechanisms and characterize how the price index reaches equilibrium states.

Complex networks consist of a natural preference for the study of real-world complex systems, such as climate analysis, biological neural connections, the World Wide Web, public transportation, airline networks, financial markets, and social networks (29–38). In this context, random graph networks describe the topology of a set of N nodes connected with chance p, thus introducing a fundamental probability distribution across graphs. The Erdös-Rényi algorithm is a well-known method for the assembly of random graph networks as it connects an initial set of N isolated nodes by adding a total of $pN(N-1)/2$ random links between them while forbidding double connections (39, 40).

In Fig. 1, we illustrate the Erdös-Rényi process of building a random graph network with $N = 10$ and $\langle k\rangle = 3$. We also present the averaged degree distribution $P(k)$ over ten networks with $N = 2\times10^4$ nodes and several values of $\langle k\rangle$. The lines correspond to Poisson fits for the data with average degree $\langle k\rangle = pN$, in agreement with the degree distribution of random graphs for large networks.

Modern financial markets operate as a complex system, the dynamics of which depend on not only the rational strategy of the individual but also the emotional circumstances that define the psyche of the investor. At first, individual decisions might seem challenging to model; nevertheless, social agents tend to follow herding behavior, as they feel sheltered when the crowd endorses their choices. In this way, trader social dynamics are reasonably attainable (14, 15).

In financial markets, the bias to follow a significant group is often embraced by less experienced agents, denoted as *noise traders*, who buy (sell) when other agents are buying (selling). Noise traders are highly susceptible to the dominant opinion and overreact to fresh news regarding buying or selling. In contrast, other traders, denoted as *noise contrarian traders* or *fundamentalists*, tend to follow the global minority in a given market as an investment strategy, buying (selling) when the market majority is selling (buying). Conversely, fundamentalists buy when stock prices decline and sell when prices increase (10–13). Therefore, their decision-making process drives the asset price toward its fundamental value.

The remainder of this paper is organized as follows. In *Model*, we describe the global-vote opinion formation model for financial markets and present the relevant quantities analyzed in our simulations. In *Results and Discussion*, we present the numerical results obtained along with the corresponding discussions.* Finally, *Conclusions and Final Remarks* summarizes our investigation.

*Data provided by Yahoo Finance.

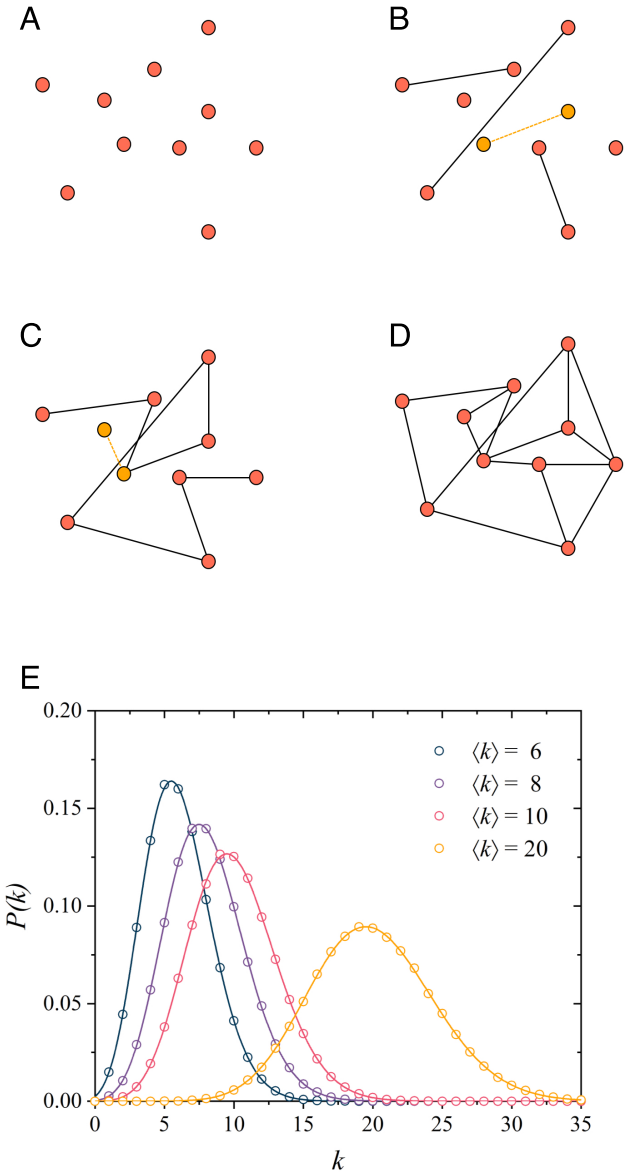

Fig. 1. Illustration of the Erdös-Rényi process of building random graph networks. From (*A*) to (*D*), $N = 10$ isolated nodes are connected by adding a total of $pN(N-1)/2 = 15$ random links between them while forbidding double connections. The final network has $\langle k\rangle = 3$. In (*E*), we show the degree distribution $P(k)$ averaged over ten networks for $\langle k\rangle = 6, 8, 10$, and 20 with $N = 2\times10^4$. The lines represent Poisson fits for the data.

1. Model

A. Financial Interactions. We represent financial agents on the market and their interactions using a complex network structure. We place N agents on the nodes of a random graph network, where the links represent the interactions between agents in the market. We map the agent's financial decision (opinion or option) at a given time t by a spin variable, which may assume one of two values, $+1$ or -1, regarding buying or selling an asset. Furthermore, to model the essential dynamics of real-world financial markets, we randomly distribute two sets of individuals: a fraction, $1-f$, of noise traders and the remaining fraction, f, of fundamentalist traders, also referred to as noise contrarians. We use the spin variables λ and α to represent the financial options of noise traders and contrarian agents, respectively.

B. Market Anxiety. We introduce a noise parameter variable, q, to model the level of economic anxiety and perceived uncertainty present in the market. This work considers that market apprehension relates to the chance for an agent to perform an incorrect economic action. We assume the same level of market anxiety q for contrarian and noise traders' agents, where q represents the probability of an agent choosing the opposite of its standard strategy when negotiating in the financial market.

C. Noise Traders. An individual noise trader, i, with opinion λ_i, assumes the same opinion of the majority of its neighbors with probability $1-q$ and the opposite option with probability q. We write the opinion flipping probability for noise trader agent i as follows:

$$\omega(\lambda_i) = \frac{1}{2}\left[1-(1-2q)c_\lambda \lambda_i \mathrm{sgn}(m_i)\right], \qquad [1]$$

where $\mathrm{sgn}(x) = -1, 0, +1$ for $x < 0$, $x = 0$ and $x > 0$, respectively. Here, c_λ stands for the agent strategy, where we set $c_\lambda = +1$ to model the trend among noise traders to agree with the local majority of their neighbors. Variable m_i quantifies the local predominant opinion, or local magnetization, defined as

$$m_i = \sum_{\delta=1}^{k_i} \lambda_{i+\delta}. \qquad [2]$$

The summation runs over all k_i neighboring agents connected to the trader at node i. From Eq. **1**, it can be seen that when $q = 0$, the noise trader adopts its local predominant opinion. When we increase the market anxiety parameter q, the noise trader tends to follow the opposite opinion of its local majority, rejecting its standard strategy and, thus, making an investment mistake.

D. Noise Contrarians. A fundamentalist agent tends to follow the market minority opinion with probability $1-q$ while following the majority opinion with chance q. We define the prevailing option of the system as global magnetization, which influences the financial opinion of noise contrarian traders. The option of a noise contrarian agent j, α_j, flips with the following probability:

$$\omega(\alpha_j) = \frac{1}{2}\left[1-(1-2q)c_\alpha \alpha_j \mathrm{sgn}(M)\right], \qquad [3]$$

where c_α is defined as fundamentalists' strategy, and since these individuals tend to agree with the global minority of the system, $c_\alpha = -1$ for all noise contrarian agents.

Variable M measures the average market option of the system, thus revealing the economic order. Magnetization M accounts for the financial opinion of every agent in the market and is evaluated as

$$M = \frac{1}{(N_\lambda + N_\alpha)}\left(\sum_{i=1}^{N_\lambda}\lambda_i + \sum_{j=1}^{N_\alpha}\alpha_j\right), \qquad [4]$$

where $N_\lambda = N(1-f)$ stands for the number of noise trader agents in the network and $N_\alpha = Nf$ represents the number of noise contrarian agents. For $M = 1$, every agent on the market has an option equal to $+1$. Similarly, $M = -1$ denotes a market configuration where every agent opinion is equal to -1. $M = 0$ represents the case where half of the agents have opinion $+1$ and the other half have opinion -1. Additionally, intermediate values of M infer the dominant opinion of the market.

We remark that when $q = 0$, a contrarian agent always follows the opposite opinion of global magnetization: the agent buys (sells) when the majority sells (buys). As q increases, there is a greater probability of the contrarian agent following the majority, adopting the opposite of his or her inherent financial market strategy.

In the global-vote model for financial markets, we recover the standard MVM on random graphs when the fraction of contrarians f is zero (20). In this case, we observe an order-disorder phase transition at a critical point, q_c, for each value of average connectivity $\langle k\rangle$ in the thermodynamic limit $N \to \infty$. This $f = 0$ system presents an ordered phase, with large clusters of agents that share the same opinion for values of noise q below the critical point q_c. By increasing q, the same opinion clusters fade, and the magnetization (order parameter) approaches zero.

In this work, we analyze the global-vote model for financial markets on random graphs for several values of average connectivity $\langle k\rangle$ and the fraction of noise contrarian traders $f \neq 0$. We set q near $q_c(\langle k\rangle, f = 0)$ to model real-world market dynamics adequately since previous investigations have suggested that a strong market phase emerges when the system is close to its critical melting point for the $f = 0$ case (1, 2, 10). In this work, we adopt the notation $q_c(\langle k\rangle)$ to represent $q_c(\langle k\rangle, f = 0)$.

2. Results and Discussion

We perform Monte Carlo simulations on Erdös-Rényi random graphs of size N = 10,201 and different values of average connectivity $\langle k\rangle$. For the network of financial interactions, we randomly place a fraction, $1-f$, of noise traders on the network nodes and occupy the remaining fraction f with noise contrarian agents. In this way, $N = N_\lambda + N_\alpha$.

This work considers that a real-world market presents a small fraction of noise contrarian agents. To this extent, we investigate the influence of noise contrarian agents for q near its critical value for the $f = 0$ case, obtained in previous studies within several values of $\langle k\rangle$ (20), with our model exhibiting key real-world market features (1, 2). Additionally, we consider small values for the average number of connections of an agent in a market, i.e., small values of $\langle k\rangle$, supported by the agreement between the data of real-world markets and the results of our simulations.

Market dynamics evolve as follows. We randomly select an agent and update its opinion accordingly with the probabilities given by Eqs. **1** and **3** for a noise trader and a noise contrarian agent, respectively. We repeat this process N times, thus defining a unity of time in one Monte Carlo step (MCS). This way, each agent's opinion is updated once, on average, in one MCS. To discard the transient regime, we allow this dynamic to run during 10^3 MCS, and we perform our analysis in the subsequent 10^5 MCS.

In the financial context, we relate global magnetization M, or the order parameter of the system, to the aggregate excess demand of a particular asset to identify its impact on stock prices. Market demand depends on the investors' perception of the market, and the model embraces the premise that the demands of investors drive price changes with an infinite speed of price adjustment or instantaneous price updates (28). Thus, a positive demand ($M > 0$) causes prices to rise, while a negative demand ($M < 0$) causes prices to fall, and markets that fluctuate around the equilibrium exhibit average excess demand that oscillates around zero. Therefore, we consider magnetization as a measure of price (1, 2, 10–14).

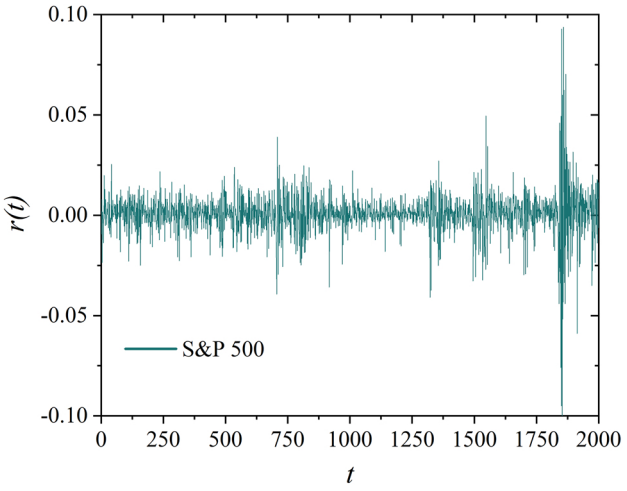

Fig. 2. Logarithmic returns for the daily closing price of the S&P 500 index in US dollars from November 01, 2012, to December 08, 2020. The high volatility observed for the period around t = 1,850 represents the COVID-19 stock market crash of 2020.

To investigate intermittent market dynamics, we quantify the logarithmic return at a given time t as follows:

$$r(t) = \log\left[\left|M(t)\right|\right] - \log\left[\left|M(t-1)\right|\right]. \qquad [5]$$

The financial return time series represents the price variation in a given asset over time. Positive (negative) returns relate to profit (loss) during the period of analysis.

In Fig. 2, we present the logarithmic return for the closing values of the S&P 500 index in US dollars from November 01, 2012, to December 08, 2020. Similar to any other traditional asset, the S&P 500 index depends mainly on market supply and demand, a fundamental financial mechanism that yields several periods of strong return variations. Periods of significant return fluctuations are compressed in time, denoting the clustered volatility effect for the analyzed index price. This financial phenomenon is known as volatility clustering, and it can be elucidated by Mandelbrot's observation that "large changes tend to be followed by large changes—of either sign—and small changes tend to be followed by small changes" (41).

Fig. 2 also shows that the period around t = 1,850 presents the most considerable time-series return volatility, denoting the COVID-19 pandemic phase, where government officials halted economic activity. The panic and uncertainty triggered by the financial impacts of such measures led to an expressive stock market crash (42, 43).

In Fig. 3, we analyze the influence of the average connectivity $\langle k\rangle$ and noise contrarian fraction f on the market order of the model on random graphs. Fig. 3*A* exhibits two distinct market phases: a "strong market phase" for $f = 0.20$ (dark blue), where the system is highly volatile and magnetization exhibits an irregular wave pattern, and a "weak market phase" for $f = 0.70$ (yellow), where magnetization values are approximately randomly distributed (1, 2). This result demonstrates that the increase in the number of contrarian agents tends to stabilize market dynamics, where highly volatile periods are present but to a substantially lower extent. Additionally, the increase in the agent's average number of connections $\langle k\rangle$ and noise parameter q also yields stochastic patterns of market demand but drives a contraction in the amplitude of these fluctuations, as observed in Fig. 3*B* (18–20).

Fig. 4 displays the logarithmic returns of the absolute value of the order parameter. In financial markets, we define volatility as a measure of the variation around the average returns observed in an asset's time series. In this figure, we note intensive market fluctuations for $f = 0.20$, embodied by the large spikes shown in the plot. This result also shows clustered volatility, a real-world market feature. We observe that the presence of contrarian agents tends to stabilize the market, as indicated by attenuated fluctuations in returns. It becomes clear that increasing the average connectivity of the network and the market noise parameter similarly increases the number of events of high volatility while simultaneously reducing clustered volatility, deviating from the expected behavior from the expected of real-world financial markets. Fig. 4*A* shows that periods of high volatility tend to be clustered for lower values of f, providing a more adequate representation of real-world market dynamics (41).

To quantify the effects of volatility clustering, we compute the autocorrelation of absolute returns as follows:

$$A(\tau) = \frac{\sum_{t=\tau+1}^{T}\left[\left|r(t)\right| - \left|\bar{r}\right|\right]\left[\left|r(t-\tau)\right| - \left|\bar{r}\right|\right]}{\sum_{t=1}^{T}\left[\left|r(t)\right| - \left|\bar{r}\right|\right]^2}, \qquad [6]$$

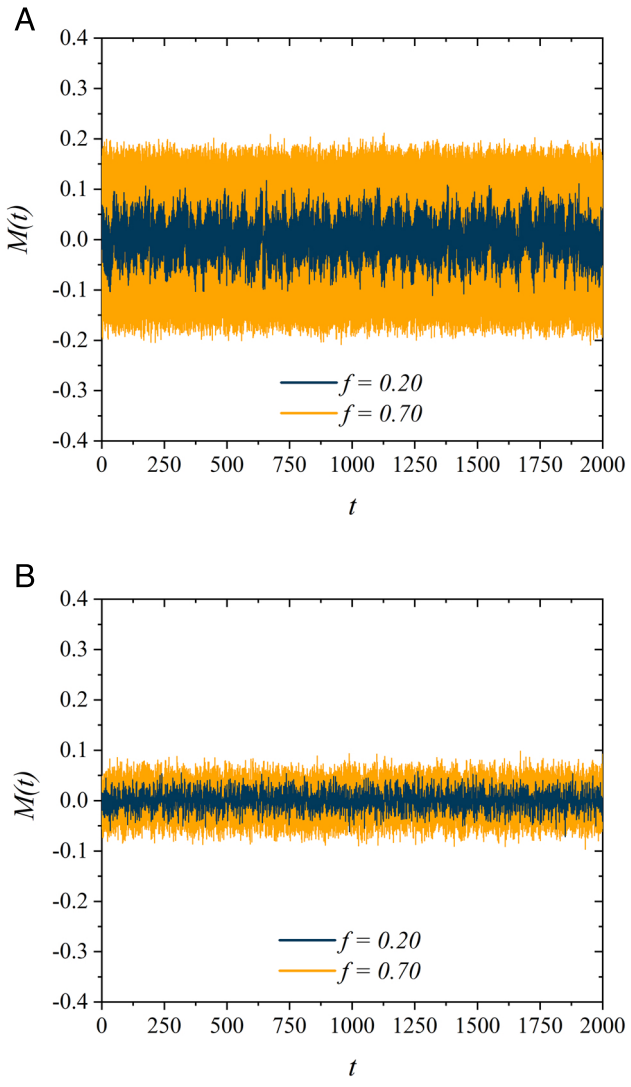

Fig. 3. Time series of the order parameter M for two sets of parameters: (*A*) $\langle k\rangle = 6$ for $q = 0.240$, and (*B*) $\langle k\rangle = 50$ for $q = 0.411$.

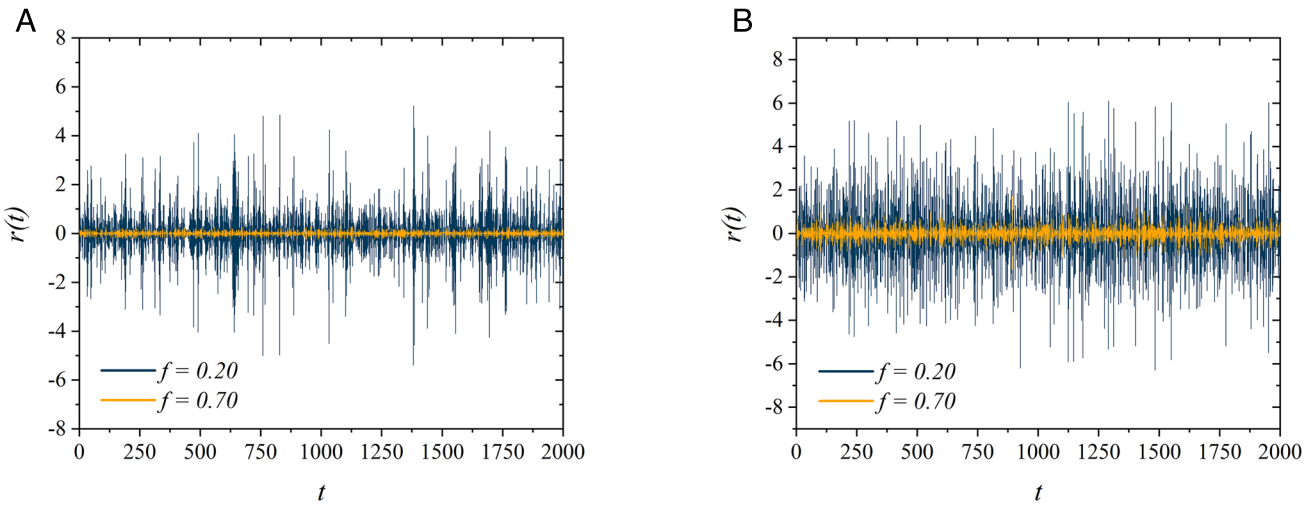

Fig. 4. Logarithmic returns of the absolute magnetization for (*A*) $\langle k \rangle = 6$ and $q = 0.240$, (*B*) $\langle k \rangle = 50$ and $q = 0.411$.

where $1 \leq \tau \leq 10^5$ MCS is the time-step difference between observations, $T = 10^5$ MCS is the time of simulation, $r(t)$ is the return at time t, and $\bar{r}$ is the average value of the return. The function defined by Eq. **6** measures nonlinear correlations between observations of the absolute value of log-returns as a function of the time delay separating them.

Fig. 5 displays the autocorrelation for several values of f, showing that the returns present a strong correlation in time with exponential decay (1, 2, 10, 12, 13). To illustrate this exponential behavior, we perform an exponential fit of the autocorrelation function $A(q, f, t) \sim \exp(-t/t_0)$ for $f = 0.20$ and $\langle k \rangle = 6$, and we obtain $t_0 \approx 1.5 \times 10^8$ MCS. Other values for the fraction of noise contrarian agents f and small $\langle k \rangle$ yield similar results.

In Fig. 6, we compare the results of our model with real-world financial indices. We calculate the autocorrelation function for the daily log-returns of the closing values of the indices: Dow Jones (DJI, observed from January 29, 1985, to December 02, 2020), Ibovespa (BVSP, July 24, 1993, to December 02, 2020), Nikkei (N225, January 05, 1980, to December 02, 2020), S&P 500 (GSPC, January 02, 1985, to December 02, 2020), and Nasdaq (IXIC, October 01, 1985, to December 02, 2020). We analyze each index for approximately 7×10^3 d and use $1 \leq \tau \leq 7 \times 10^3$. We note that the returns for each investigated index display an expressive correlation that decays exponentially over time.

Fig. 7 displays the histogram of the log-returns for $\langle k \rangle = 6$ and several values of the noise contrarian fraction f in 10^5 MCS. Real-world market systems display fat-tailed distributions as a reflection of lower nonzero probabilities of obtaining above- or below-average returns. We observe such behavior only for lower values of the fraction of contrarians f, substantiating a real-world market region for our agent-based dynamics. To quantify the return distributions, we perform a statistical analysis of the data. We obtain that kurtosis $\mathrm{K}(\langle k \rangle, f)$ for $f = 0.20$ (strong market phase) is $\mathrm{K}(6, 0.20) = 5.85$ and $\mathrm{K}(8, 0.20) = 4.98$. For $f = 0.70$ (weak market phase), $\mathrm{K}(6, 0.70) = 2.41$ and $\mathrm{K}(8, 0.70) = 2.37$. We remark that for a normal distribution $\mathrm{K} = 3$, increasing the fraction of contrarian agents f gradually shifts the system's behavior from a leptokurtic (fat-tailed) regime to a mesokurtic (Gaussian) regime.

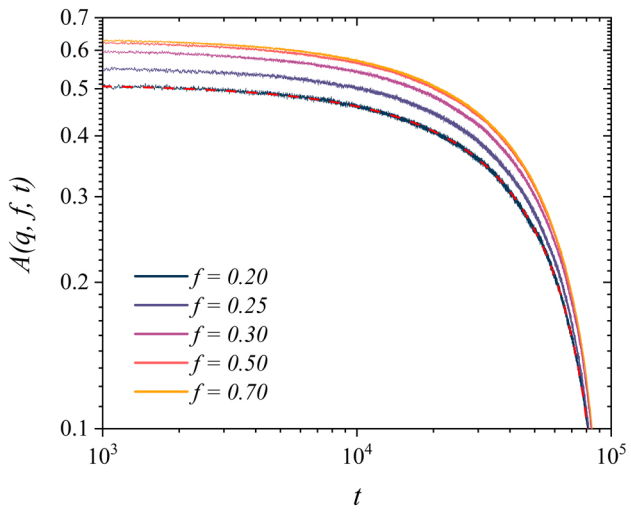

Fig. 5. Log-log plot of the autocorrelation of absolute logarithmic returns for $\langle k \rangle = 6$ and $q = 0.240$. The dashed red line represents exponential fit for the data.

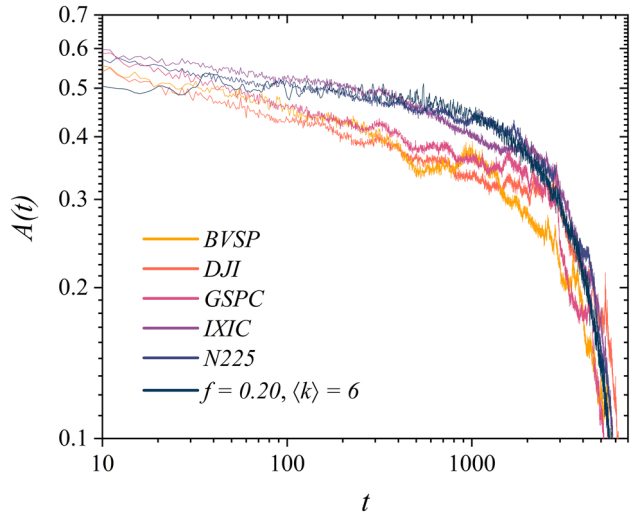

Fig. 6. Log-log plot of the autocorrelation of absolute logarithmic returns of the closing values for several financial indices and for $\langle k \rangle = 6$, $q = 0.240$ with $f = 0.20$ (dark blue).

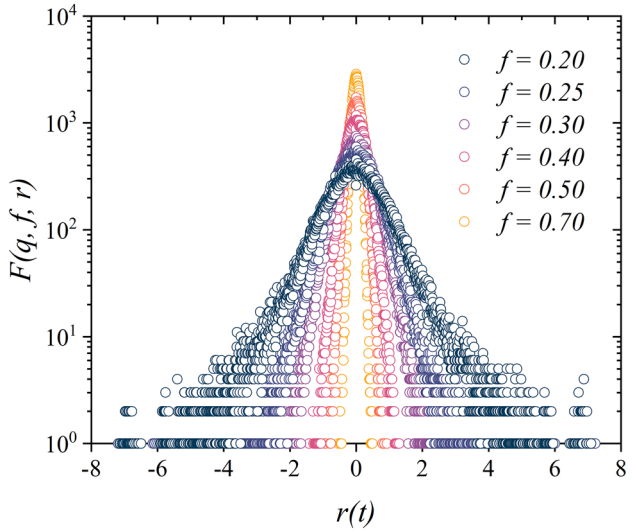

Fig. 7. Distribution of logarithmic returns in 10^5 MCS and several values of the fraction of contrarian agents f for $\langle k \rangle = 6$ and $q = 0.240$.

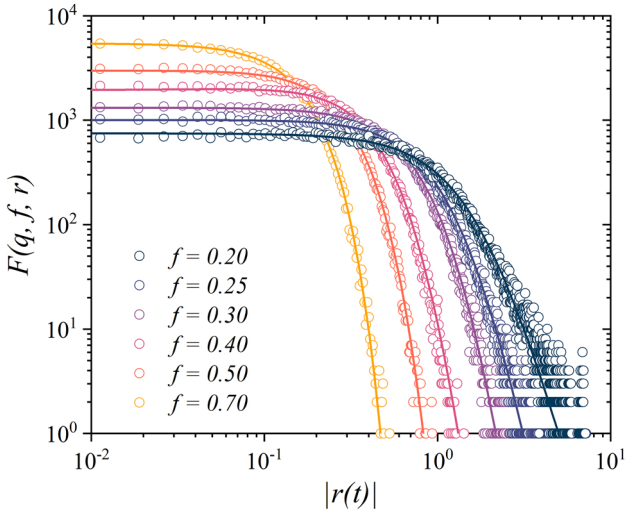

Fig. 9. Plot of the absolute log-return distributions $F(q, f, r)$ for several values of fraction f with $\langle k \rangle = 6$ and $q = 0.240$ in 10^5 MCS. The lines for $f \leq 0.40$ correspond to Student's t fits, whereas the lines for $f \geq 0.5$ correspond to Gaussian fits.

To qualify the distributions of Fig. 7, we perform a comparative normal quantile–quantile (Q–Q) plot. Fig. 8 displays the Q–Q plots for the distribution of log-returns using several values for the fraction of fundamentalists f. The red line represents the expected results of a Gaussian distribution, and if a particular distribution exhibits similar behavior, then its data points should lie on that reference line. For lower values of f, for instance, $f \leq 0.40$, Fig. 8 displays nonlinear behavior in the Q–Q plot, thus indicating that the distributions of log-returns feature fat tails and, therefore, are non-Gaussian. In such distributions, a greater chance of obtaining higher-than-expected return values for normal distributions is observed, consistent with real-world market systems (3).

Fig. 9 displays the probability distribution of the absolute log-returns for several values of f in 10^5 MCS with $\langle k \rangle = 6$. We find that Student's t distributions can depict the phase data of the strong market ($f \leq 0.40$), while those of the weak market are well fitted by Gaussian distributions (1, 2). Assuming that the mean values μ of the distributions are zero, as illustrated by Fig. 10, we perform generalized Student's t fits for the data $S(r; \nu, \mu, \sigma) = S(r; \nu, \sigma)$, where ν is the degree of freedom and σ represents the scale. Function S is defined as follows:

$$S(r; \nu, \sigma) = \frac{1}{\sqrt{\nu\sigma^2}\,\mathrm{B}\left(\frac{\nu}{2}, \frac{1}{2}\right)} \left(1 + \frac{r^2}{\nu\sigma^2}\right)^{-\frac{\nu+1}{2}}, \qquad [7]$$

where

$$\mathrm{B}\left(\frac{\nu}{2}, \frac{1}{2}\right) = \int_0^1 t^{\frac{\nu}{2}-1}(1-t)^{-\frac{1}{2}}\,\mathrm{d}t, \qquad [8]$$

is the beta function (44, 45). The values obtained for the degree ν and scale σ are displayed in Table 1. As the fraction of contrarian agents increases, we find that the absolute log-return distributions are well fitted by a Gaussian distribution $g(r)$ as follows:

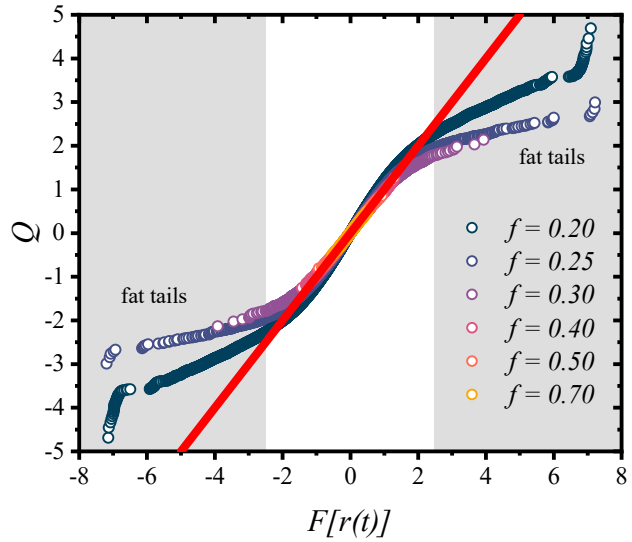

Fig. 8. Normal quantile–quantile plots of the logarithmic return distributions for $\langle k \rangle = 6$ and $q = 0.240$ in 10^5 MCS.

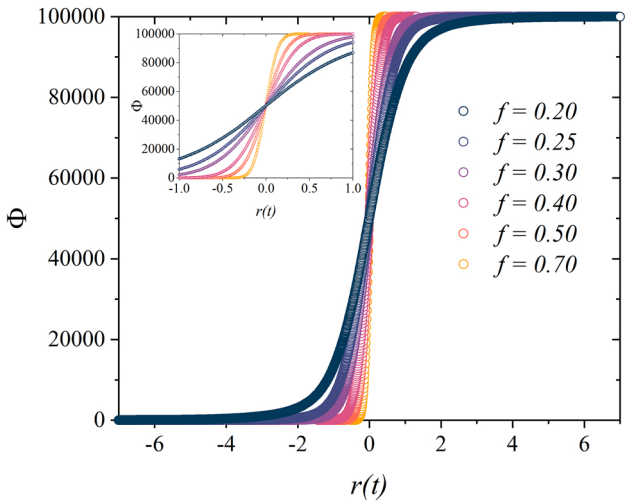

Fig. 10. Plot of the cumulative distribution Φ of log-returns in 10^5 MCS for $\langle k \rangle = 6$ and $q = 0.240$. The inset shows the details for $r(t)$ near 0.

Table 1. Correlation between the scale σ and degree ν as a function of the fraction of contrarian agents f, average connectivity $\langle k\rangle$, and noise q

	$\langle k\rangle = 6$, $q = 0.240$		$\langle k\rangle = 8$, $q = 0.275$	
f	ν	σ	ν	σ
0.20	5.0(3)	0.80(1)	3.0(1)	0.785(8)
0.25	7.4(5)	0.558(6)	6.3(4)	0.621(6)
0.30	12(2)	0.444(6)	10(1)	0.559(8)
0.40	13(2)	0.252(5)	38(2)	0.319(6)

$$g(r) = \frac{1}{\sigma\sqrt{2\pi}}\, e^{-\frac{1}{2}\left(\frac{r-\mu}{\sigma}\right)^2}, \qquad [9]$$

where σ is the SD, and μ is the mean, which we again consider to be zero. In Table 2, we display Gaussian fit information.

Fig. 10 displays the cumulative distribution of logarithmic returns Φ for the data in 10^5 MCS, from which we imply that the mean of the distributions remains zero for $\langle k\rangle = 6$ with $q = 0.240$ for several values of f.

Table 2. Dependence of SD σ on the fraction f, on average connectivity $\langle k\rangle$, and on noise parameter q

	$\langle k\rangle = 6$, $q = 0.240$	$\langle k\rangle = 8$, $q = 0.275$
f	σ	σ
0.50	0.1916(8)	0.2254(9)
0.70	0.1108(4)	0.1284(5)

In Fig. 11, we show the distribution of the absolute log-returns of the closing values of several financial indices to the results found in our investigation. We analyze each index for approximately 7×10^3 d and use Student's t distributions to fit the data, represented by the lines in the plots. In Table 3, we show the values for degree ν and the scale σ. We note that the degree of freedom determines primarily the shape of each distribution, and a comparison shows that our model behaves as expected for real-world

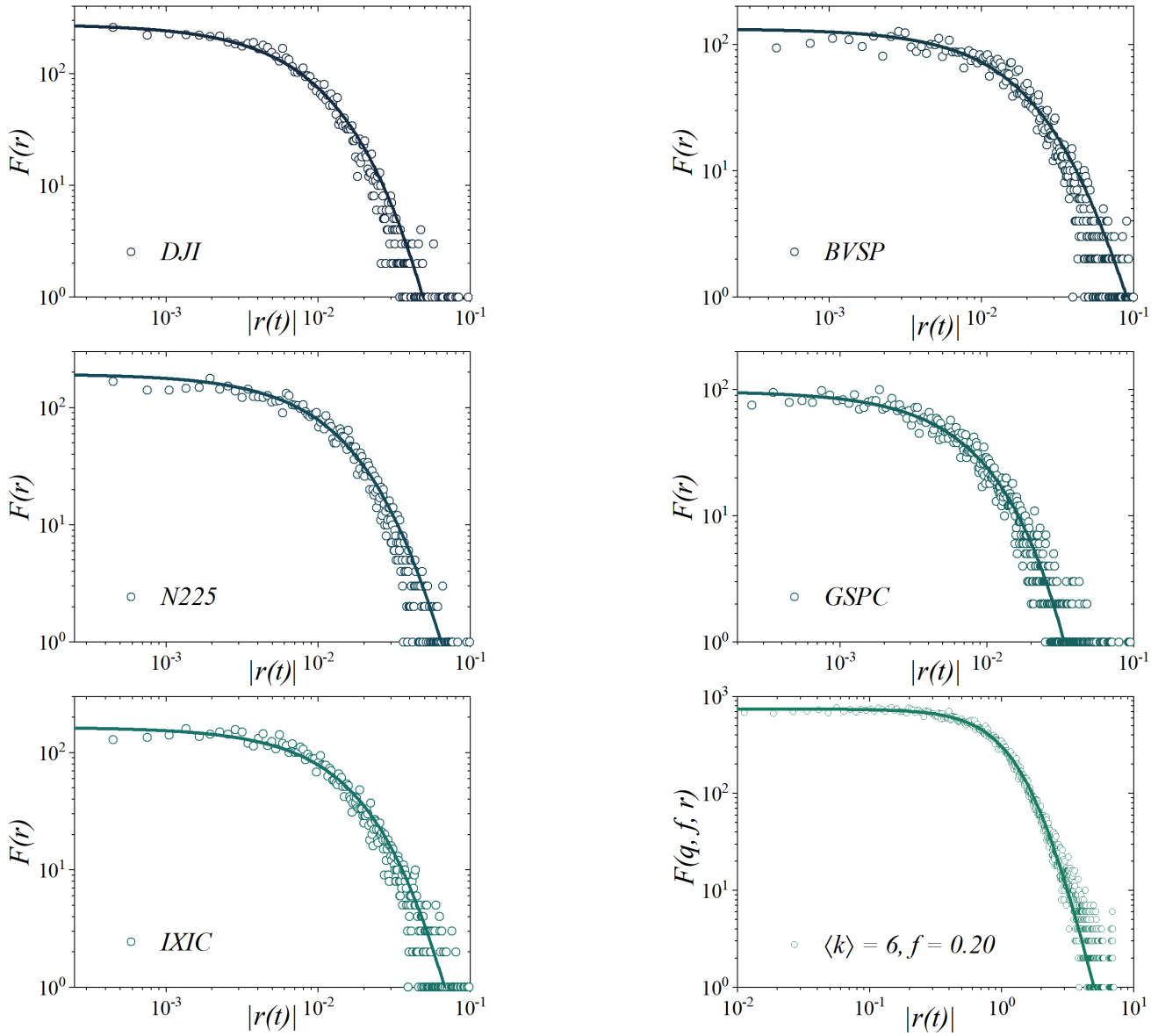

Fig. 11. Plot of the absolute log-return distributions $F(r)$ of the closing values for several financial indices and the absolute log-return distributions for $\langle k\rangle = 6$, $q = 0.240$, and $f = 0.20$. The lines correspond to Student's t fits.

Table 3. Scale σ and degree ν for absolute log-return distributions of several financial indices with Student's t fits

Index	ν	σ
Dow Jones	9.5(2)	0.01248(8)
Ibovespa	4.2(3)	0.0197(6)
Nikkei	15.3(6)	0.0202(2)
S&P 500	15.6(5)	0.0151(1)
Nasdaq	6.5(3)	0.0180(3)

financial markets. In contrast, the scale parameter measures fluctuations around the mean of the distribution, and comparison displays a disparity in the order of magnitude obtained in the fits. By analyzing Figs. 2 and 4, we observe that the daily log-returns of financial markets are one order of magnitude smaller than those obtained in our simulations and thus account for the divergence in the results. Hence, we observe that our model represents real-world financial market behavior in a satisfactory manner.

We also perform an extensive investigation of the model for several values of average connectivity $\langle k\rangle$ and different values of noise q. Fig. 12 displays a multiplot table of the histograms of logarithmic returns for several $(q, f, \langle k\rangle)$ triplets. Columns correspond to values of q, below criticality $q < q_c(\langle k\rangle)$ (*Left*), at criticality $q = q_c(\langle k\rangle)$ (*Center*) and above criticality $q > q_c(\langle k\rangle)$ (*Right*). In this work, we use the values of $q = q_c(\langle k\rangle)$ obtained in previous investigations of the MVM on random graphs, where the fraction of contrarian agents f is set to zero (20). The values of noise above and below criticality are taken to be $q_c(1 \pm 10\%)$.

We observe that distributions exhibit fat tails for lower values of f, especially for small values of $\langle k\rangle$ (i.e., $\langle k\rangle = 6$ and $\langle k\rangle = 8$), and at its corresponding critical value of q. In contrast, such behavior is lost for higher values of the average connectivity and values of q that deviate from criticality. This result illustrates and supports our choice for $\langle k\rangle$ and q_c used in this investigation.

We conclude that the adoption of random graph networks in the global-vote model for financial markets has been demonstrated to be effective. Our model is able to both qualitatively and quantitatively reproduce real-world market features for lower values of the average connectivity $\langle k\rangle$, a small fraction of fundamentalist agents f and near criticality $q(\langle k\rangle) = q_c(\langle k\rangle)$.

We remark that other combinations of values for $\langle k\rangle, f$, and q might yield similar results. Nevertheless, our particular approach adopts simple key ideas: a limited and small number of interacting agents, values of the noise parameter q near criticality, and a small number of contrarian agents in the market. Despite the model's simplicity, it has shown its capability to characterize the mechanisms that drive social behavior and decision-making in economic systems.

3. Conclusions and Final Remarks

This work proposes a generalization of the two-state global-vote model for financial markets on random networks. The global-vote model suggests that any stock market dynamics consist

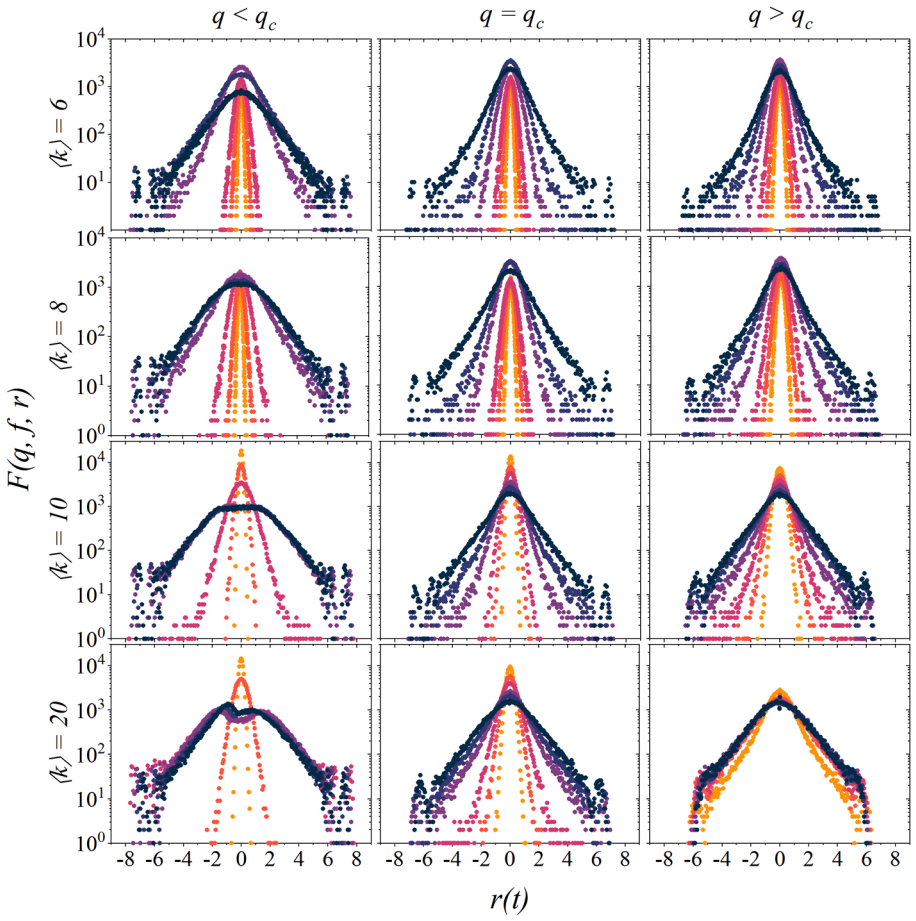

Fig. 12. Distributions of logarithmic returns in 10^5 MCS for different values of $\langle k\rangle$ in the vicinity of $q_c(\langle k\rangle)$ with several values of f: 0.20, 0.25, 0.30, 0.50, and 0.70 (dark blue, purple, violet, pink, orange, and yellow, respectively).

primarily of different agent strategies driven by economic and social interactions. In its standard version, the stock market consists of a heterogeneous population with two distinct kinds of investors: noise traders, who follow the local majority of their neighbors, and noise contrarian traders, influenced by the global minority of the system (1).

We aim to investigate the distribution dependence of the return on the average connectivity $\langle k \rangle$ of the random graph network. We relate variations in the global magnetization of the system to the daily return of a given asset. Our simulations reproduce the typical qualitative and quantitative real-world financial time series, thus, yielding key features such as fat-tailed distributions of returns, volatility clustering, and long-term memory volatility. We demonstrate that higher values for average connectivity $\langle k \rangle$ or fraction of noise contrarians f, as well as values of q far from criticality, may eliminate similar real-world behavior in our model. In these circumstances, this result suggests that economic markets function near their critical point, where opinion exchanges and local influences span the system efficiently (16–25).

The model contributes to our understanding of the rich and complex dynamics of financial markets, driven by the emotional and rational decisions of its agents, via a straightforward description. We reduce the complexities of such systems by assuming that financial markets consist of a random network of interacting agents who follow either the opinion of most of their peers or strategies of their own. Furthermore, our model outputs are comparable to real-world markets in terms of a finite socioeconomic temperature, with the most significant fraction of agents interacting with a small number of neighbors. In contrast, the remaining fraction follows the market index. We remark that this framework allows us to enrich the knowledge of such complex economic systems without using an extensive number of variables.

We expect this study to trigger further research and eventual applications. Future investigations may include inertia for the market index update to represent price trends and speculation among investors, a time-dependent interaction network, additional investment strategies, and different interaction structures, such as small-world and scale-free networks.

Data, Materials, and Software Availability. There are no data underlying this work.

ACKNOWLEDGMENTS. We acknowledge financial support from Brazilian and Chinese institutions and funding agents Universidade de Pernambuco (UPE), Fundação de Amparo à Ciência e Tecnologia de Pernambuco (FACEPE) (APQ-0565-1.05/14, APQ-0707-1.05/14), Coordenação de Aperfeiçoamento de Pessoal de Nível Superior (CAPES), Conselho Nacional de Desenvolvimento Científico e Tecnológico (CNPq) (306068/2021-4), National Natural Science Foundation of China (72071006, 61603011, 62073007). The Boston University Center for Polymer Studies is supported by NSF Grants PHY-1505000, CMMI-1125290, and CHE-1213217, by Defense Threat Reduction Agency (DTRA) Grant HDTRA1-14-1-0017, and by Department of Energy (DOE) Contract DE-AC07-05Id14517.

Author affiliations: [a]Física de Materiais, Escola Politécnica de Pernambuco, Universidade de Pernambuco, Recife, PE 50720-001, Brazil; [b]Center for Polymer Studies, Department of Physics, Boston University, Boston, MA 02215; [c]College of Economics and Management, Beijing University of Technology, Beijing, 100124, China; and [d]Photrek LLC, Watertown, MA 02472

1. A. L. M. Vilela, C. Wang, K. P. Nelson, H. E. Stanley, Majority-vote model for financial markets. *Phys. A: Stat. Mech. Appl.* **515**, 762–770 (2019).
2. B. J. Zubillaga, A. L. M. Vilela, C. Wang, K. P. Nelson, H. E. Stanley, A three-state opinion formation model for financial markets. *Phys. A: Stat. Mech. Appl.* **588**, 126527 (2022).
3. H. E. Stanley, R. N. Mantegna, *An introduction to econophysics* (Cambridge University Press, Cambridge, 2000).
4. H. E. Stanley *et al.*, Self-organized complexity in economics and finance. *Proc. Natl. Acad. Sci. U.S.A.* **99**, 2561–2565 (2002).
5. F. Baldovin, A. L. Stella, Scaling and efficiency determine the irreversible evolution of a market. *Proc. Natl. Acad. Sci. U.S.A.* **104**, 19741–19744 (2007).
6. Y. Li, A. L. M. Vilela, H. E. Stanley, The institutional characteristics of multifractal spectrum of China's stock market. *Phys. A: Stat. Mech. Appl.* **550**, 124129 (2020).
7. E. Bonabeau, Agent-based modeling: Methods and techniques for simulating human systems. *Proc. Natl. Acad. Sci. U.S.A.* **99**, 7280–7287 (2002).
8. L. Feng, B. Li, B. Podobnik, T. Preis, H. E. Stanley, Linking agent-based models and stochastic models of financial markets. *Proc. Natl. Acad. Sci. U.S.A.* **109**, 8388–8393 (2012).
9. L. Zhao *et al.*, Herd behavior in a complex adaptive system. *Proc. Natl. Acad. Sci. U.S.A.* **108**, 15058–15063 (2011).
10. S. Bornholdt, Expectation bubbles in a spin model of markets: Intermittency from frustration across scales. *Int. J. Mod. Phys. C* **12**, 667–674 (2001).
11. T. Lux, M. Marchesi, Scaling and criticality in a stochastic multi-agent model of a financial market. *Nature* **397**, 498–500 (1999).
12. T. Kaizoji, S. Bornholdt, Y. Fujiwara, Dynamics of price and trading volume in a spin model of stock markets with heterogeneous agents. *Phys. A: Stat. Mech. Appl.* **316**, 441–452 (2002).
13. T. Takaishi, Simulations of financial markets in a Potts-like model. *Int. J. Mod. Phys. C* **16**, 1311–1317 (2005).
14. R. Cont, J. P. Bouchaud, Herd behavior and aggregate fluctuations in financial markets. *Macroecon. Dyn.* **4**, 170–196 (2000).
15. K. Sznajd-Weron, R. Weron, A simple model of price formation. *Int. J. Mod. Phys. C* **13**, 115–123 (2002).
16. M. J. de Oliveira, Isotropic majority-vote model on a square lattice. *J. Stat. Phys.* **66**, 273–281 (1992).
17. M. J. de Oliveira, J. F. F. Mendes, M. A. Santos, Nonequilibrium spin models with Ising universal behaviour. *J. Phys. A: Math. Gen.* **26**, 2317 (1993).
18. F. W. S. Lima, A. O. Sousa, M. A. Sumuor, Majority-vote on directed erdős-rényi random graphs. *Phys. A: Stat. Mech. Appl.* **387**, 3503–3510 (2008).
19. P. R. A. Campos, V. M. de Oliveira, F. G. B. Moreira, Small-world effects in the majority-vote model. *Phys. Rev. E* **67**, 026104 (2003).
20. L. F. C. Pereira, F. G. B. Moreira, Majority-vote model on random graphs. *Phys. Rev. E* **71**, 016123 (2005).
21. M. A. Santos, S. Teixeira, Anisotropic voter model. *J. Stat. Phys.* **78**, 963–970 (1995).
22. A. R. Vieira, N. Crokidakis, Phase transitions in the majority-vote model with two types of noises. *Phys. A: Stat. Mech. Appl.* **450**, 30–36 (2016).
23. A. L. M. Vilela, F. G. B. Moreira, Majority-vote model with different agents. *Phys. A: Stat. Mech. Appl.* **388**, 4171 (2009).
24. A. L. M. Vilela, H. E. Stanley, Effect of strong opinions on the dynamics of the majority-vote model. *Sci. Rep.* **8**, 1–8 (2018).
25. A. L. M. Vilela, L. F. C. Pereira, L. Dias, H. E. Stanley, L. R. da Silva, Majority-vote model with limited visibility: An investigation into filter bubbles. *Phys. A: Stat. Mech. Appl.* **563**, 125450 (2021).
26. H. Hong, J. C. Stein, A unified theory of underreaction, momentum trading, and overreaction in asset markets. *J. Financ.* **54**, 2143–2184 (1999).
27. C. Chiarella, The dynamics of speculative behavior. *Ann. Oper. Res.* **37**, 101–123 (1992).
28. A. Beja, M. B. Goldman, On the dynamic behavior of prices in disequilibrium. *J. Financ.* **35**, 235–248 (1980).
29. J. H. Feldhoff *et al.*, Complex networks for climate model evaluation with application to statistical versus dynamical modeling of South American climate. *Clim. Dyn.* **44**, 1567–1581 (2015).
30. J. C. Reijneveld, S. C. Ponten, H. W. Berendse, C. J. Stam, The application of graph theoretical analysis to complex networks in the brain. *Clin. Neurophysiol.* **118**, 2317–2331 (2007).
31. A. L. Barabási, R. Albert, H. Jeong, Scale-free characteristics of random networks: The topology of the world-wide web. *Phys. A: Stat. Mech. Appl.* **281**, 69–77 (2000).
32. X. lei An, L. Zhang, Y. zhen Li, J. gang Zhang, Synchronization analysis of complex networks with multi-weights and its application in public traffic network. *Phys. A: Stat. Mech. Appl.* **412**, 149–156 (2014).
33. Y. Yu *et al.*, System crash as dynamics of complex networks. *Proc. Natl. Acad. Sci. U.S.A.* **113**, 11726–11731 (2016).
34. R. Albert, A. L. Barabási, System crash as dynamics of complex networks. *Rev. Mod. Phys.* **74**, 1723 (2002).
35. G. Dong *et al.*, Resilience of networks with community structure behaves as if under an external field. *Proc. Natl. Acad. Sci. U.S.A.* **115**, 6911–6915 (2018).
36. K. Growiec, J. Growiec, B. Kamiński, Social network structure and the trade-off between social utility and economic performance. *Soc. Netw.* **55**, 31–46 (2018).
37. T. Watanabe, A numerical study on efficient jury size. *Humanit. Soc. Sci. Commun.* **7**, 62 (2020).
38. D. Melamed, B. Simpson, B. Montgomery, V. Patel, Inequality and cooperation in social networks. *Sci. Rep.* **12**, 6789 (2022).
39. P. Erdös, A. Rényi, On the evolution of random graphs. *Publ. Math. Inst. Hung. Acad. Sci.* **5**, 17–60 (1960).
40. B. Bollobás, A. Thomason, Random graphs of small order in *North-Holland Mathematics Studies* (Elsevier, 1985), vol. 118, pp. 47–97.
41. B. Mandelbrot, The variation of certain speculative prices. *J. Bus.* **36**, 394–394 (1963).
42. M. Mazura, M. Dang, M. Vega, Covid-19 and the March 2020 stock market crash. Evidence from s&p1500. *Financ. Res. Lett.* **38**, 101690 (2021).
43. S. Fu, C. Liu, X. Wei, Contagion in global stock markets during the Covid-19 crisis. *Glob. Chall.* **5**, 2000130 (2021).
44. K. P. Nelson, S. R. Umarov, M. A. Kon, On the average uncertainty for systems with nonlinear coupling. *Phys. A: Stat. Mech. Appl.* **468**, 30–43 (2017).
45. S. Queirós, L. G. Moyano, J. de Souza, C. Tsallis, A nonextensive approach to the dynamics of financial observables. *Eur. Phys. J. B* **55**, 161–167 (2007).